

# Novel SiC UV Instrumentation Development with Potential Applications for the Habitable Worlds Observatory

**Prabal Saxena<sup>a,\*</sup>, Zeynep Dilli<sup>a</sup>, Peter Snapp<sup>b</sup>, Allison Youngblood<sup>c</sup>, Tilak Hewagama<sup>a</sup>, Shahid Aslam<sup>a</sup>, Chullhee (Chace) Cho<sup>b</sup>, Augustyn Waczynski<sup>b</sup>, Nader Abuhassan<sup>d</sup>, Ahn T. La<sup>a</sup>, Bryan K. Place<sup>d</sup>, Thomas F. Hansico<sup>a</sup>, Ryan Stauffer<sup>a</sup>, Dina Bower<sup>a</sup>, Akin Akturk<sup>c</sup>, Neil Goldsman<sup>e</sup>, Bryce Galey<sup>e</sup>, Ethan Mountfort<sup>e</sup>, Mitchell Gross<sup>e</sup>, Ryan Purcell<sup>e</sup>, Usama Khalid<sup>e</sup>, Yekta Kamali<sup>e</sup>, Chris Darmody<sup>e</sup>, Robert Washington<sup>f</sup>, Tim Livengood<sup>a</sup>, Daniel P. Moriarty<sup>a</sup>, Carl A. Kotecki<sup>b</sup>, Narasimha S. Prasad<sup>g</sup>, Joseph Wilkins<sup>f</sup>**

<sup>a</sup>NASA Goddard Space Flight Center, 8800 Greenbelt Rd, Greenbelt, MD 20771, USA

<sup>b</sup>Detectors Systems Branch, NASA Goddard Space Flight Center, Greenbelt, MD 20771, USA

<sup>c</sup>Exoplanets and Stellar Astrophysics Lab, NASA Goddard Space Flight Center, Greenbelt, MD 20771, USA

<sup>d</sup>SciGlob Instruments and Services, LLC., 9881 Broken Land Pkwy, Columbia, MD 21046, USA

<sup>e</sup>CoolCAD Electronics, Inc., 5000 College Ave Suite 2105, College Park, MD 20740, USA

<sup>f</sup>Howard University, 2400 6th St NW, Washington, DC 20059, USA

<sup>g</sup>NASA Langley Research Center, 1 Nasa Dr, Hampton, VA 23666, USA

\*Corresponding author. Email: [prabal.saxena@nasa.gov](mailto:prabal.saxena@nasa.gov)

\*Prabal Saxena, [prabal.saxena@nasa.gov](mailto:prabal.saxena@nasa.gov)

## 1 Introduction

The most recent Astrophysics Decadal Survey Report<sup>1</sup> underscored the importance of ultraviolet (UV) observations in exploring numerous high priority science questions. Ultraviolet observations are key to understanding stellar atmospheres, the morphology and dynamics of galaxies, the interaction of black holes with their surroundings and the properties of worlds outside our solar system, including their potential habitability. This is merely a subset of areas where UV observations are key, and such observations were also recognized as an essential means of achieving the objectives of the Report's top flagship priority, the Habitable Worlds Observatory (HWO). The driving exoplanet and cosmological objectives of HWO require observations in the UV range of 100 – 320 nm using normal incidence optics.<sup>2</sup> These observations will require high-sensitivity UV detectors that can probe challenging observational targets at levels that require technological and engineering advancement. In this paper we detail recent and current work that is being carried out to fabricate

and advance novel SiC UV instrumentation that is aimed at enabling more sensitive measurements across numerous disciplines, with a short discussion of the promise such detectors may hold for HWO.

The near-ultraviolet (NUV) spectral region (170-320 nm) is a subset of the ultraviolet spectral region that contains many powerful tracers of atoms, molecules, and small particulates such as dust and hazes. These NUV tracers have wide-ranging applications across numerous disciplines, such as Astrophysics, Planetary Science, Heliophysics, and Earth Science. Briefly, SiC detectors are a potentially powerful future technology in these other non-Astrophysics disciplines. With respect to Planetary Science, SiC detectors hold the potential to significantly improve measurements (1 order of magnitude improvement in signal-to-noise ratio (SNR) compared to state-of-the-art (SOA) silicon-based focal plane arrays)<sup>3</sup> for UV spectroscopy of comet coma and planetary atmosphere and aurora studies relevant to key planetary decadal objectives.<sup>4</sup> SiC detectors can also enable new measurements of molecules on bodies that are episodically sourced from plumes, for example, measurements of airglow emission when Io is in shadow (which could not historically be observed, due to the long accumulation time and contamination from scattered light from Jupiter) and could reveal the relative effects of SO<sub>2</sub> frost and SO<sub>2</sub> gas photoabsorption.<sup>5</sup> With respect to Heliophysics, SiC detectors have the potential to serve as radiation particle detectors in sun observations that require blindness to interfering visible and longer wavelength UV photons.<sup>6</sup> Lastly, applications specific to Earth Science include enabling ground/space-based passive remote sensing of trace gases and aerosols of interest by eliminating the need to conduct optical light filtering,<sup>7</sup> which can interfere with accurate chemical retrievals by adding fringe structures to collected spectra that can obscure weaker chemical signatures. While SiC detectors have numerous other potential uses in all of these disciplines, this study focuses on technology development and application to an HWO

astrophysics use case.

With respect to Astrophysics, SiC detectors have the potential to provide a wide range of sensitive, enabling observations of interest, including UV spectroscopic measurements of active galactic nuclei, exoplanet host stars, and gravitational wave sources. SiC detectors directly satisfy the need for high-quantum efficiency (QE), solar-blind, broad-band NUV detectors identified in Astrophysics Biennial Technology Report 2022.<sup>8</sup> In fact, the highest priority science areas from the Astrophysics Decadal Survey Report<sup>1</sup> all benefit from sensitive NUV observations. For example, the NUV is a critical bandpass for distinguishing between physical models<sup>9</sup> of the extremely hot and rapidly evolving kilonova that emerges in the seconds to hours after the merger of two neutron stars. Additionally, in the search for habitable exoplanets, the Hartley-Huggins ozone band in the NUV is the most sensitive tracer of oxygenic atmospheres.<sup>10</sup> Obtaining information regarding these atmospheres is complicated by the high contrast ratios between the host star and planet and the low amount of reflected light from potential exo-Earth candidates. To enable significant breakthroughs in these areas, next generation detectors must maximize in-band sensitivity while minimizing noise. For imaging applications, minimizing responsivity to longer wavelength light is essential because many astrophysical sources are orders of magnitude brighter in the optical than the NUV. SiC is known to possess many of these properties<sup>3</sup> and with the advancement of fabrication techniques, is now being explored by our team as a potential option for many of these use cases.

Our team is pursuing fabrication of SiC instruments relevant to numerous disciplines under multiple projects funded by NASA's Science Mission Directorate (SMD) and Space Technology Mission Directorate (STMD), as well as through Small Business Innovation Research Grants and through NASA Goddard's Internal Research And Development program. The PReSSiC (Planetary

Remote Sensing using SiC detectors) project is building, testing and validating a High Sensitivity Silicon Carbide Focal Plane Detector that would be optimized for miniaturized instrumentation that can be part of planetary science missions, including cubesats. The focal plane assembly is being designed so that it can obtain radiance observations with a higher detectivity than previous generations of NUV spectrometers from 200-340nm at a  $R \sim 200$ . This is with the goal of being able to obtain remote sensing observations of targets in the NUV with a (SNR)  $> 10 \times$  better than current leading detectors from identical observational platforms. Key science motivation in this project is understanding the hydration state of planetary bodies across the solar system, with a specific focus on the Moon and the identification of outgassed (non-water related) volatiles, characterization of atmospheric constituents and hazes and understanding of the mineralogy of airless bodies. Simultaneously, an ongoing development effort is the NASA STMD Early Career Initiative supported “Design of a Broad Utility, Visible-Blind, SiC, UV Spectrometer for Astrophysics, Planetary and Earth Science Applications, Validated Through Representative Measurement of Climate Forcing Gases” project, hereafter referred to as the Pandora-SiC effort, which aims to achieve clean differential optical absorption spectroscopy measurements of columnar trace gases in the earth atmosphere in the 280-450 nm regime through integration of visible blind UV detectors, produced by leveraging recent advances in SiC fabrication, into an existing, ground-based, atmospheric spectroscopy platform, Pandora.<sup>11</sup> SiC instrument development is also being carried out under other grants, including the Ultra-Violet Detector Innovation for Raman Exploration and Characterization (UV-DIRECT) of Ocean Worlds project. UV-DIRECT aims to enable identification of minerals, volatiles, organic molecules, biopolymers, water, and other hydrous phases in planetary materials by fabricating a SiC avalanche photodiode (APD), with high internal gain, specifically targeted for the identification of ocean world-relevant compounds. UV-DIRECT is be-

ing carried out in collaboration with Army Research Labs and is developing a detector that would use UV/NUV (266-340 nm) Raman spectroscopy with ppb sensitivity to achieve these planetary science observations. While a range of SiC instrumentation development is being carried out by our team, we will focus on the PReSSiC and Pandora-SiC plans and development in this paper and how advancements in these projects may be beneficial for future potential Astrophysics applications.

Section 2 describes key background information on SiC as a semiconductor material, with a brief discussion of comparison to other materials. Section 3 lays out planned and current development work in the key SiC instrument development projects that are in progress. Section 4 provides updates on fabrication and integration progress of the photodetectors for the corresponding projects. Section 5 discusses results and updates on recent and current testing of photodetector properties and also describes planned future work. Finally, Section 6 incorporates these SiC detector properties into a simulation of potential exoplanet observations by HWO using SiC detectors and also discusses potential application to HWO.

## 2 Background on SiC

Work on the development of highly sensitive wide energy band gap ( $E_g$ ) UV-EUV detectors at NASA Goddard Space Flight Center (GSFC) started more than two decades ago,<sup>3</sup> particularly in direct band gap material AlGaN ( $E_g = 3.4 - 6.2$  eV)<sup>12-14</sup> and indirect band gap material 4H-SiC ( $E_g = 3.2$  eV)<sup>15,16</sup> material systems with successful fabrication of photodiodes demonstrating good performance characteristics.<sup>3,17</sup>

For NASA, these wide energy band gap devices offered several key advantages for space applications over conventional Si ( $E_g = 1.1$  eV) based devices, such as:

- visible-blind detection,
- high thermal stability,
- better radiation hardness,
- high breakdown electric field,
- high chemical inertness, and
- greater mechanical strength.

Furthermore, the shorter cut-off wavelength of these material systems eliminates the need for bulky and expensive optical filtering components, mitigating risk and allowing for simpler optical designs of instrumentation.

A compelling reason for using wide-band gap semiconductors for UV detectors is the low dark currents that can be attained. The dark current, under zero or reverse bias conditions in the depletion region of a semiconductor, is determined from the rate of generation ( $G$ ) of electron-hole pairs:

$$G = \frac{n_i}{\tau}$$

where  $n_i$  is the intrinsic carrier concentration and  $\tau$  is the effective recombination lifetime. The intrinsic carrier concentration is given by:

$$n_i = N_v N_c \exp\left(-\frac{E_g}{2kT}\right)$$

where  $N_v$  is the valence band density of states,  $N_c$  is the conduction band density of states,  $E_g$  is the energy band gap,  $k$  is the Boltzmann constant, and  $T$  is the temperature. The dark current

density,  $J_d$ , is directly proportional to  $n_i$  and is given by:

$$J_d = \frac{qn_iW}{\tau}$$

where  $q$  is the electronic charge, and  $W$  is the depletion width. For silicon at room temperature,  $n_i$  halves for every 9 K decrease in temperature. By comparison, a wider band gap semiconductor with the same density of states and  $\tau$  as silicon, but a 0.036 eV higher band gap, achieves the same factor of two reduction in  $n_i$ . The exponential dependence of  $n_i$  on band gap makes a 0.12 eV increase in band gap equivalent to a 30 K temperature drop, both offering an order-of-magnitude reduction in thermal generation rate. Wide-band gap semiconductors achieve significantly lower thermally generated dark current due to 10 or more orders of magnitude reduction in  $n_i$ , even in the presence of large differences in  $\tau$ . Furthermore, wide-band gap semiconductors exhibit strong temperature dependence, indicating that moderate cooling can significantly reduce the dark current.

Wide-band gap semiconductors are appealing for detecting UV-A (315–400 nm), UV-B (280–315 nm), UV-C (200–280 nm), and EUV (1–125 nm) radiation since they are inherently visible blind. The reduced need for blocking filters increases the system quantum efficiency (QE) and simplifies optical systems. Compared to narrow band gap materials, wide-band gap semiconductors are significantly more radiation tolerant, making them excellent candidates for space applications.

SiC detectors have several advantages over Si detectors:

1. Wide Bandgap: The band gap of 4H-SiC is 3.2 eV, three times wider than Si. Its intrinsic carrier density is  $10^{20}$  times lower than that of Si, leading to significantly lower dark current.

2. Visible Blindness: SiC detectors are visible-blind, enabling UV, EUV, and X-ray photon detection without interference from visible or IR backgrounds.
3. Excellent Rigidity: SiC has high displacement energy ( $\sim 21$  eV) compared to Si (12 eV), offering superior radiation hardness.

While AlGaN provides the advantage of direct band gap heterostructures, SiC has greater material maturity. For example, the defect density of SiC ( $10^{-10}$ – $10^3$ /cm<sup>3</sup>) is several orders of magnitude lower than GaN ( $10^6$ – $10^{10}$ /cm<sup>3</sup>). Recent developments in SiC avalanche photodiodes (APDs) have enabled high-performance devices for UV detection. Zhou et al.<sup>18</sup> demonstrated  $1 \times 128$  linear arrays of 4H-SiC UV APDs with high pixel yield (100%), uniform breakdown voltage with a variation of 0.2 V, quantum efficiency (QE) of 53.5% at 285 nm, and dark currents below 1 nA at 95% of breakdown voltage.

Similar materials proposed for UV detection including indium gallium nitride (InGaN),<sup>19</sup> Diamond,<sup>20</sup> and zinc oxide (ZnO)<sup>21</sup> suffer from similar lack of material maturity. With respect to another similar material, SiC may be able to provide improved measurements compared to current state of the art (SOA) delta-doped silicon CCDs utilized on missions like SPARCS (>4 times improved out of band rejection without a need for additional filters).<sup>22</sup> Much of this is because SiC substrate and epi-growth technologies have developed to such a level as to allow the fabrication of many different types of SiC photodetectors with desired features.<sup>23</sup> SiC UV p-i-n photodiodes have already been fabricated and are commercially available. SiC avalanche photodiodes with extremely high gain and low excess noise have also been demonstrated. For additional information on the progress and history of SiC fabrication and use in many other applications, see.<sup>23</sup>

### **3 Overview of development activities**

SiC instrument development by our team under the current programs have leveraged the expertise of scientists, engineers and commercial companies with fabrication, integration and implementation expertise. Key to the fabrication tasks across all the project is the work that CoolCAD Electronics, LLC, has been carrying using unique expertise in the design and fabrication of devices and integrated circuits with SiC. CoolCAD has previously worked on SiC low-power CMOS, deep-UV sensors, and building blocks for deep-UV-sensitive focal plane arrays as well as high-power, high-voltage and high-temperature SiC devices. CoolCAD's current work to obtain UV sensors and readout circuitry on the same substrate leverages background work supported by NASA SBIR programs (NNX17CG32P, "Silicon Carbide 10 $\mu$ m-Pitch UV Imaging Array and APD with Active Pixel Readout," Phase 1 SBIR; NNX16CG51P, "Single Chip EUV, VUV, and Deep UV Photodetector System with Integrated Amplifier," Phase 1 SBIR; NNX17CG15C, "A Silicon Carbide Foundry for NASA's UV and High Temperature CMOS Electronics Needs," Phase 2/2E SBIR). CoolCAD has fabricated/demonstrated two classes of UV sensor devices and structures, both of which are top-lit: PN-junction and Schottky diodes and SiC UV Focal Plane Arrays, which are the focus of the current projects. The spectral responsivity is partially dependent on depth of the photocurrent-collecting junction electric field. Schottky diodes, with the built-in field closest to the surface, are expected to show a responsivity peak with a shorter wavelength, which has been observed in the devices. CoolCAD employs implant profile engineering, to set the implant energies and doses necessary to achieve a desired profile, which has also been incorporated in current work. Finally, both past GOES-R funding and a current IRAD has supported demonstration of the radiation hardness and visible blind nature of the SiC material that is relevant to all of the projects

under development.

The PReSSiC project aims to deliver a lab-tested  $1 \times 128$  pixel 4H-SiC detector suitable for spectrometers in miniaturized platforms that can obtain radiance observations with a higher detectivity than previous generations of NUV spectrometers from 200-340nm at a  $R \sim 200$ . Key development for this project has been testing a number of design trades and optimizing design and fabrication for this goal. The project has begun with a focus on design and layout of individual sensors and small arrays. Potential single-pixel geometries and fabrication parameters are being evaluated to optimize device characteristics such as responsivity and response speed, which will be examined in the context of the science requirements. A key area of exploration is a test of implant depth, as it is valuable to create an implant profile which supports enhanced sensitivity in the spectral region of interest. There are limits on this process, such as difficulty of getting implants past a certain depth into the tough SiC crystal material. An additional consideration is that in a focal plane array, the pixels must be electrically and optically isolated for clear image formation - deep isolation trenches. CoolCAD Electronics has previously demonstrated small-pixel-count 2-D arrays with  $10 \mu\text{m}$  pitch, that had not featured deep trench isolation, but is examining deep isolation trenches in the new arrays.

The project is laying out and fabricating a number of different test structures and small-pixel-count arrays to identify potential fabrication difficulties and limits to our fabrication techniques. Diode pitch will be varied between 6-40  $\mu\text{m}$  and the project is looking at a number of factors including: contact resistance, minimum trench width for effective fill and planarization, patterning long metal Lines, surface leakage reduction, and effects on responsivity and dark current. The team has also started examining packaging and I/O structure design for both active and passive pixels. The team is designing and building a set of readout electronics, particularly for planned scaling up

of the pixel count for the full array. Radiometric testing is being conducted and will be conducted at numerous steps along the way and a testbed is currently being assembled so that the arrays can eventually be tested under both ambient and vacuum conditions. Key performance testing related to responsivity, noise performance and dispersion will be compared to requirements based upon simulations.

Another key ongoing development effort is the NASA Early Career Initiative-supported “Design of a Broad Utility, Visible-Blind, SiC, UV Spectrometer for Astrophysics, Planetary and Earth Science Applications, Validated Through Representative Measurement of Climate Forcing Gases” project, hereafter referred to as the Pandora-SiC effort, which aims to achieve clean differential optical absorption spectroscopy measurements of columnar trace gases in the earth atmosphere in the 280-450 nm regime. This is accomplished through integration of visible blind UV detectors, produced leveraging recent advances in SiC fabrication, into an existing, ground-based, atmospheric spectroscopy platform, Pandora,<sup>11</sup> which has been developed by a commercial partner, SciGlob, LLC. The ECI Team is hoping to improve the reliability and temporal resolution of total column formaldehyde measurements conducted by Pandora either for direct data collection or validation for data collected from satellite platforms like the ozone monitoring instrument (OMI).<sup>24</sup> A simultaneous goal of this project is also to simplify instrument setup through elimination of filter components, enabled by the visible blindness of SiC, and reducing or eliminating cooling requirements, enabled by the large bandgap and therefore reduced dark current of SiC. The ECI effort is at the point of integrating fabricated SiC detectors,  $1 \times 128$  and  $1 \times 1024$  arrays of high aspect ratio ( $25 \mu\text{m} \times 200 \mu\text{m}$ ,  $25 \mu\text{m} \times 500 \mu\text{m}$ , and  $50 \mu\text{m} \times 500 \mu\text{m}$ ), passive, P-on-N photodiodes with external capacitive transimpedance amplifier (CTIA) read-out integrated circuits (ROIC) configured to be controlled by an external imaging array controller. Following integration, detector units will

be tested to confirm quantum efficiency (QE) greater than 0.1 at 345 nm and dark currents  $< 20$  pA (individual diodes probed so far show a dark current upper limit of  $< 6$  fA, discussed in section 5), and integrated into the Pandora spectrometer.

The current detector and electronics configuration for both the PReSSiC detectors and the Pandora-SiC detectors has been tailored for easy integration into planetary science instruments and Pandora instrument systems, respectively. While not directly applicable to HWO, testing of pixel design, properties and layout in the PReSSiC project and maturation of the integration scheme developed through the ECI effort both provide key technology and engineering advancement for potential HWO detectors. Achieving desired noise characteristics, responsivity, and validating operation of SiC detectors using standard read out techniques offers a compelling platform for operation of denser and higher dimensionality SiC photodiode arrays of interest for use in potential Coronagraph, Spectrograph, and High Resolution Imaging Instruments.

#### **4 Fabrication and Integration Progress of Photodetectors**

For the PReSSiC and ECI projects, many of the initial tasks are focused on design and fabrication, and CoolCAD is working on a variety of linear photodiode structures in order to map the design space, identify design best practices, and optimize fabrication techniques.

Diode geometry is the first aspect being explored. For the particular spectroscopy application targeted by the ECI program, the pixel pitch required for the target spectral resolution is  $25 \mu\text{m}$ . The optical design of the instrument can take advantage of pixels with high aspect ratio. Therefore the initial fabrication run of the program includes pixels with  $25 \mu\text{m} \times 500 \mu\text{m}$  and  $25 \mu\text{m} \times 200 \mu\text{m}$  drawn areas, along with test structures with a different aspect ratio. Figure 1 shows micrographs from the fabrication process of these designs, defining different diode regions. In the context of

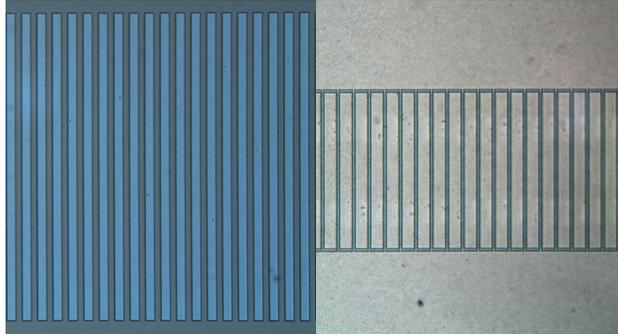


Fig 1: Micrographs from the process of different diode regions being defined by ion implantation for the tall, narrow aspect ratio diodes being developed for spectroscopy applications for the ECI program.

the PReSSiC program, a major program target is miniaturization to a very small pixel pitch and the devices being fabricated for this program include diodes with pitches as small as  $10\ \mu\text{m}$  and  $6\ \mu\text{m}$ . Figure 2 shows fabrication micrographs of some of these structures. Other geometric features being explored are the placement and sizes of contacts and interconnects, to evaluate certain trade-off aspects such as fill factor vs. diode series resistance.

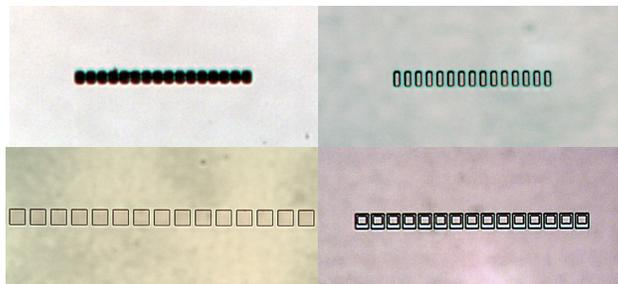


Fig 2: Micrographs from the process of different diode regions being defined by ion implantation for diode arrays with different pixel pitch for the PReSSiC project, targeting diode miniaturization.

Another aspect is different junction structures. We are fabricating pn-junction diodes with different doping profiles for these two programs, which will yield different geometries and depths for the photocurrent collection regions. For a separate NASA SBIR program, we are also fabricating Schottky diodes, which have the photocurrent collection region starting at the illuminated surface. Since shorter wavelengths have larger absorption coefficients and smaller absorption depths, the

different doping profiles are expected to have somewhat different spectral responsivity. Planned further developments include the use of different epitaxial structures for diode fabrication as well.

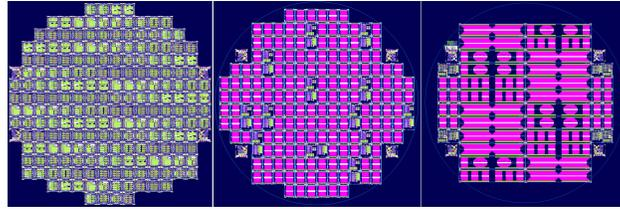


Fig 3: The wafer-scale layouts for the PReSSiC project fabrication run (left) and the ECI program fabrication run (middle, right).

For applications which use diode arrays, such as spectroscopy or imaging, pixel-to-pixel isolation can be required. For the ECI program, deep trenches between the photoactive regions of each diode are being implemented for this purpose. For the PReSSiC program, in addition to trenches, we are also implementing array variations using a specific diode geometry which was first tested for this purpose in another development program. This alternative approach allows us to increase the fill factor, especially of the smallest diodes. The development and evaluation of these isolation structures are being pursued in the SBIR program as well.

Figure 3 shows the wafer-scale designs for the initial runs in the PReSSiC project and the ECI program. The PReSSiC program design includes small-pixel-count arrays (15x1 and 8x1) and single test diodes. The ECI program design includes 128x1 and 1024x1 arrays and single test diodes. Both designs are currently in fabrication and have been through their implant schedule and isolation trench formation. We are working on the back-end processing, which comprises the metallization steps for contact metal and interconnect formation.

For both projects, the next stage of development will include active diode arrays, for which the first stage of a readout circuit converting the photocurrent to a voltage level over an integration period is fabricated on the same die with the photodiode arrays. CoolCAD Electronics has active

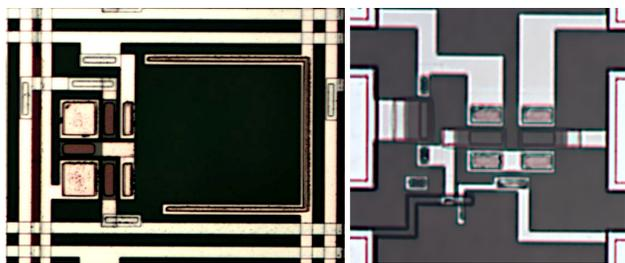
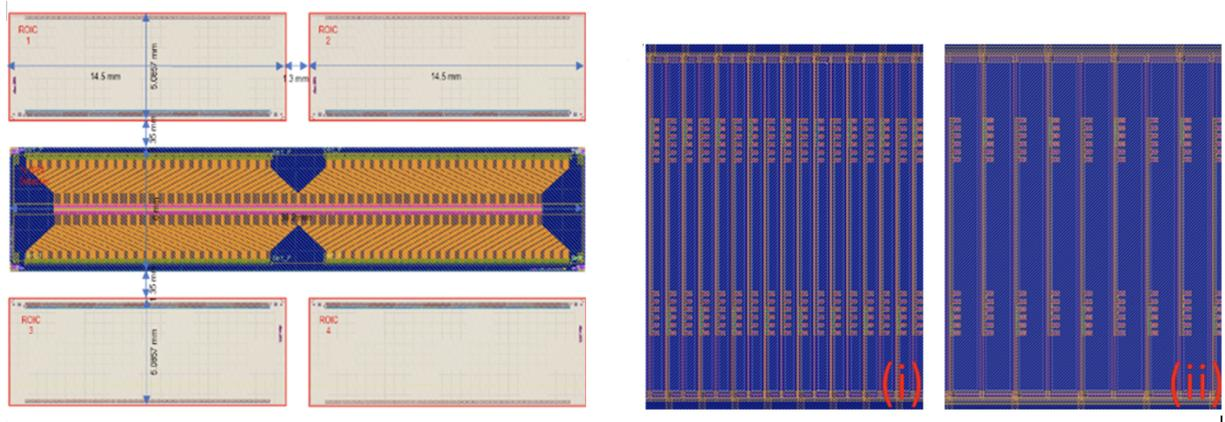


Fig 4: Previously fabricated photodiodes integrated with the first stage of a readout circuit on the same SiC die.

development programs on SiC MOSFET structures and circuits and has previously demonstrated single diodes integrated with this readout circuit. Figure 4 shows previously-fabricated examples of this structure. These development programs all start from the level of physics-based semiconductor device modeling and simulations, and include process simulation and development efforts as well as device and circuit design, layout, and fabrication. For the PReSSiC project, in addition to one-dimensional arrays for spectroscopy, two-dimensional arrays will also be implemented for push-broom spectroscopy and imaging applications. The pixel count will be expanded as well. In the SBIR program, CoolCAD is further developing larger scale two-dimensional arrays, both of passive and active pixels. For the two-dimensional active array development, this effort includes work to miniaturize the transistors as well to be able to integrate the circuit for each pixel within the pixel, since scaling a 2-D array to significant pixel counts can be impractical otherwise.

The ECI effort is focused on a short-term field demonstration of SiC focal plane arrays in an existing atmospheric spectroscopy system, Pandora, for formaldehyde detection. As a result, the selection of diode array formats was informed by the need for a mature and highly reliable diode design, the ability to interface with external readout circuitry without complex hybridization techniques, and operability at low bias levels.

This all needs to be achieved while still allowing for modification of diode structure and pitch to



(a) SiC arrays matched to readout electronics (b) SiC diodes with different pitches and aspect ratio  
 Fig 5: The structure of SiC photodiode-based focal plane arrays for the ECI effort consists of: (a) A core  $1 \times 1024$  array of SiC photodiodes, which fans out to wirebond pads matched to the inputs of wire bondable ROICs. In this case, the array is interfaced with 4 CTIA ROICs, each with 256 inputs. (b) The ECI effort is currently in the process of characterizing multiple diode variants, including: (i) arrays with a  $25 \mu\text{m}$  pitch, and (ii) arrays with a  $50 \mu\text{m}$  pitch.

achieve the necessary diode height to interact with the full spill of light from the Pandora grating and achieve high enough spectral resolution for accurate capture of formaldehyde transmission signals. To that end, mature 1D arrays of P-on-N photodiodes with electrical contacts on their upper surface that can fan out to wire bond pads matched to external readout electronics were selected (Figure 5a).

$N^+$  and  $N^-$  implant variations are being evaluated to balance depletion region depth, and therefore responsivity, with serial resistance for optimized performance. Within these constraints, diode arrays with lateral pitches of  $25 \mu\text{m}$  (Figure 5b i) and  $50 \mu\text{m}$  (Figure 5b ii) and heights of  $200 \mu\text{m}$  to  $500 \mu\text{m}$  are being fabricated to best balance the total active area ( $\sim 75\%$  active area for  $25 \mu\text{m}$  pitch devices due to the surface metallization cover,  $\sim 85\%$  active area for  $50 \mu\text{m}$  pitch devices) and spatial resolution during final applications in the field.

To speed delivery, the ECI effort has relied on fully passive photodiode arrays with each diode fanning out to a wirebond output pad, which can then be connected to the wirebond input pad of

a corresponding ROIC. In this case, a set of four commercial CTIA CMOS readouts with wire bondable inputs is used (Figure 5a). ROICs will be situated on a basic PCB with output-boosting operational amplifiers to allow operation by an external commercial imaging array controller.

While this is a simple approach to readout, it is an ideal starting point for developing readouts for more complex SiC arrays, as SiC can be read with biases consistent with those already matured for silicon detectors ( $\leq 2$  V) with sufficient responsivity to fill detector wells in a reasonable exposure time. This includes generalization to reading out 2D SiC arrays with similar top-side fanout structures, as will be tested in the PReSSiC effort.

This approach can be further generalized to readout using commercial 2D ROICs with the maturation of top-illuminated SiC detector arrays with through-chip vias for electrical integration,<sup>25</sup> or backside-illuminated SiC detectors<sup>26</sup> electrically integrated using flip-chip, indium bump bonding techniques.

## **5 Current Testing of Photodiode Properties and Near Term Future Work**

Our team has conducted initial characterization and testing of diodes during the development and fabrication process. Of note is that since much of the work is still in early stages, these photodiode characteristics are not yet optimized and in some cases bounds that do not capture the expected or even current performance of photodiodes due to evaluation techniques or hardware. This section describes some of the tests that have been conducted already and notes their limitations where applicable.

In order to achieve high-quality Formaldehyde trace signature retrieval using the Pandora platform for the ECI effort, individual photodiodes in the arrays described previously must meet minimum performance requirements. In particular, a minimum quantum efficiency (QE) of 0.14 at

300 nm is necessary to accumulate sufficient signal within a reasonable acquisition time for the selected ROIC, and dark current must be below 20 pA to achieve an appropriate signal-to-noise ratio.

Preliminary testing on isolated large photodiodes ( $0.505 \text{ mm}^2$ ) with implant structures similar to those targeted for the ECI effort (with different profiles) meet or exceed these requirements, achieving a QE of 0.1 at 345 nm, with QE increasing as the wavelength shortens (Figure 6a, measurements performed at 0 V bias). Performance is even more promising in terms of dark current. Extracting dark noise from a long-time measurement of photodiode current under dark conditions (Figure 6b, data collected at 0 V bias) establishes a ceiling on dark current of approximately 6 fA, without any cooling or additional stabilization. This performance should allow for signal-to-noise ratios in excess of 1172 during measurement.

Moving forward, analysis of dark current and QE will be expanded by probing detectors coupled to the selected ROIC with integration capability, allowing for more accurate quantification of dark current. This step is essential for accurately assessing the utility of SiC photodiodes in astrophysics applications.

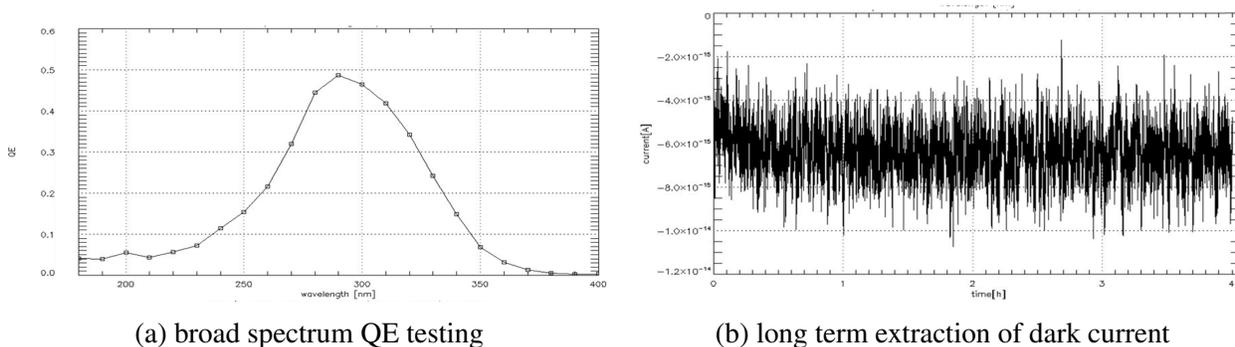
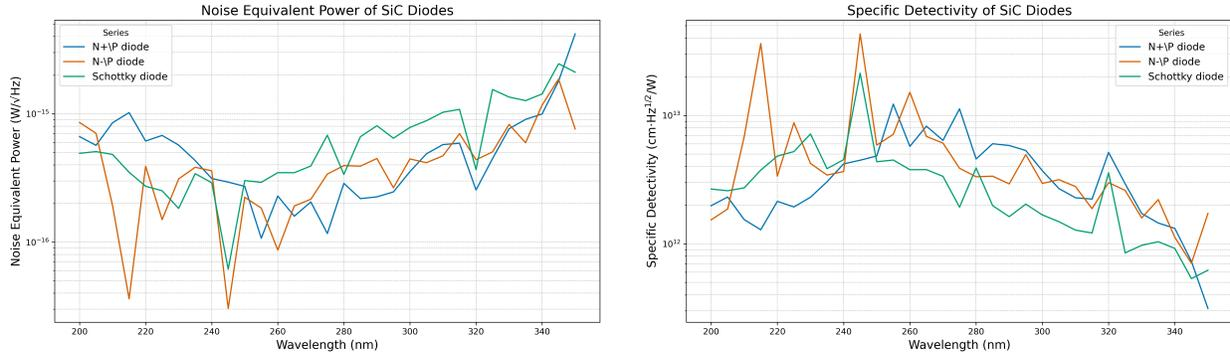


Fig 6: Characterization of large format SiC photodiodes for ECI effort including (a) broad spectrum quantum efficiency characterization and (b) dark current measurement. Additional development work is expected to improve QE values though current values already satisfy Pandora-SiC goals, while dark current is an upper bound on the true value given measurement limitations.

Similarly, initial testing of the I-V curves and QE has been conducted for photodiodes designed under an SBIR program that can be thought of as a precursor to the PReSSiC photodiodes. Under this program, three different diodes that had been fabricated were tested. The first is an  $n^+p$  diode, the second an  $n^-p$  diode and the third, a Schottky diode. The  $n^+p$  and  $n^-p$  diodes are both 40- $\mu\text{m}$  pitch diodes with exposed active areas of about  $172.5 \times 10^{-6} \text{ mm}^2$ . The Schottky diode is also a 40- $\mu\text{m}$  pitch diode with an exposed active area of  $270 \times 10^{-6} \text{ mm}^2$ . I-V curves were constructed by taking current and voltage values under illumination from 200-350nm, in 5nm increments. Quantum efficiency values were also calculated for all three diodes in the same wavelength range.

QE values for the  $n^+p$  diode peaked at 0.8 at 260nm, were above 0.6 from 240-280nm and were above 0.2 from 200 to 330nm. QE values for the  $n^-p$  diode peaked at a little bit above 0.8 at 260nm, were nearly at or above 0.6 from 230 to 290nm and were above 0.2 for a similar wavelength range as the  $n^+p$  diode. QE values for the Schottky diode peak from 250-260nm at nearly 0.7, were 0.6 or higher from 230-270nm and were above 0.2 from 200-320nm. Optical I-V curves exhibited a similar shape and general trend across all three diodes, though we note there was an offset in voltage where current approached zero which was likely due to an instrumental effect. Using the dynamic resistance calculated from the I-V curves and the QE values, we were able to calculate Specific Detectivity ( $D^*$ ) and Noise Equivalent Power (NEP) values for each of the diodes over the 200-350nm wavelength range.

The values for NEP and  $D^*$  for the diodes are given in Figure 7a and 7b. The three diodes exhibit broadly the same relationships and trends versus wavelength, with the  $n^+p$  and  $n^-p$  diodes yielding slightly lower NEP values. The 230-300 nm range possess the most favorable noise characteristics across all three diodes with a drop off in sensitivity towards longer wavelengths. While these measurements are important initial characterization steps for development of these detectors,



(a) Noise Equivalent Power of SiC Diodes

(b) Specific Detectivity of SiC Diodes

Fig 7: Comparison of NEP and Specific Detectivity of SiC Diodes.

we note they are minimum bounds on sensitivity of the diodes (put another way, they are an over-estimate of noise). This is because measurements of the I-V curve were done at coarse spectral resolution, and more highly sampled measurements where current drops to zero are likely to yield even lower dynamic resistance values for the diodes. In addition to the measurement improvements in both ECI and the SBIR/PReSSiC characterization efforts, we note that in both cases these are early stage diodes in the development process. We expect that as design and fabrication processes mature, NEP and  $D^*$  values are likely to improve.

Future characterization and testing includes both improvements to both testing methodology and hardware as well as additional tests that correspond to future development needs. Enabling very low current measurements and carrying these measurements out at highly sampled voltage values near a current minima are high near-term priorities for our team. In the future, as additional diodes are available for testing in our upcoming production runs, we will conduct additional tests to optimize diode parameters prior to focal plane array/spectrometer design. Once that is achieved, and a focal plane array/spectrometer is fabricated, our team will utilize pre-existing optical testbeds for the Pandora-SiC and PReSSiC projects to carry out instrument testing.

## 6 A promising detector material for the Habitable Worlds Observatory

The Habitable Worlds Observatory (HWO) is recommended in the most recent astrophysics Decadal Survey<sup>1</sup> to support broad coverage of 100 nm - 2.5  $\mu\text{m}$  wavelength through a variety of instrument modes, including high-contrast direct imaging of circumstellar material and bodies through coronagraphy, high angular resolution imaging, integral field spectroscopy, multi-object spectroscopy, and single-object spectroscopy. NUV capability of each of these modes is required to drive advances in our understanding of exoplanet atmospheres, stars, interstellar medium, galaxies, and solar system science. At this early stage in the mission concept design, the HWO Technology Maturation Project Office has adopted instruments from the LUVOIR-B mission concept<sup>27</sup> as a starting design and is additionally considering a UV coronagraph instrument (G. Arney, private communication). There are no requirements yet for these instruments, but based on the LUVOIR report, there is a clear need for large format arrays that are buttable on three sides and have high quantum efficiency, low dark current, and low read noise. Some instrument modes may not require large format arrays but may have more stringent requirements on efficiency and noise. The LUVOIR telescope was planned to be actively controlled to an operating temperature of 270 K and had set limits on mass and power for different observatory segments.<sup>28</sup> SiC detectors have potential to satisfy or achieve many of these requirements and desired properties.

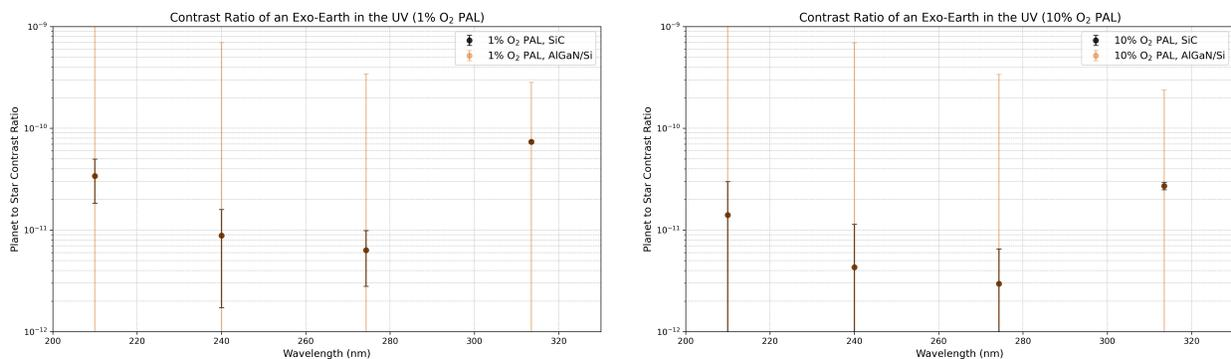
The key scientific motivation for the UV coronagraph is to search for ozone on potentially habitable exoplanets. Ozone is a significant biosignature on the Earth, because it is generated from the photolysis of oxygen by UV sunlight. The Hartley-Huggins band of ozone between 200-350 nm is much stronger than the Chappuis band near 600 nm and would be a sensitive tracer of ozone at levels significantly lower than present day values. This is key because oxygen and consequently

ozone are likely to have varied significantly over Earth's history, and over much of the Earth's past are likely to have been at much lower levels than present day values. For example, prior to the great oxygenation event, around 1-2 billion years ago, the abundance of oxygen in Earth's atmosphere is likely to have been only 0.1% of present-day levels.<sup>29</sup> Current oxygen and ozone levels are a relatively recent feature of Earth's atmosphere, and consequently, there is increasing recognition that sensitivity to smaller abundances of the two molecules is desirable when probing whether a world may be habitable. Thus, NUV spectroscopy is a powerful probe of smaller amounts of ozone, that may enable characterization of a planet's habitability even when key biosignature gases are at abundances significantly lower than present day Earth's abundances.

To demonstrate the promise of SiC detectors for HWO, we describe a use case of measuring ozone in an Earth-like exoplanet with the UV coronagraph in comparison to other potential detector material. We assume the UV coronagraph would be operable over the 225-450 nm range, but with a smaller instantaneous bandpass and optimized for 250 nm. We focus on the 210-350 nm range that captures contributions from the ozone signatures in the longer wavelength portion of that region and that aligns with wavelength regions of focus for the two projects detailed in previous sections. We assume we are observing a potential exo-Earth candidate at a distance from Earth that corresponds to the Tau Ceti system. Multiple HWO target lists indicate that such a system would have favorable observational properties for HWO,<sup>30</sup> including completeness of systems' habitable zone<sup>31</sup> (though we note there are likely even more favorable systems that are closer to Earth).

We take atmospheric profiles for the simulated planet from Whole Atmosphere Community Climate Model—WACCM6 runs that simulate atmospheres relevant to previously inferred states of the Earth atmosphere prior to the present day.<sup>32</sup> We specifically choose oxygen and corresponding ozone profiles from the 1 and 10% O<sub>2</sub> PAL simulations - these scenarios match the range of

expected abundances for much of the Proterozoic and Phanerozoic eras, which cover more than half of Earth’s history. We note that while corresponding values are taken for ozone and oxygen, we do not self-consistently model the chemical abundances of other low or trace abundance atmospheric constituents. Most of these gases are not abundant enough to impact spectra, particularly in the near-ultraviolet, and are consequently not as critical to the goals of our simulation for this paper. However, we do intend to incorporate chemically self-consistent atmospheres in future work. Spectra of the planet is modeled using the Planetary Spectrum Generator (PSG).<sup>33</sup> Using PSG, we simulate spectra of the system as viewed edge on with the planet at quadrature, with sampling techniques and radiative transfer details given in previous work.<sup>34</sup>



(a) Simulated HWO Spectra for a 1% O<sub>2</sub> PAL Case (b) Simulated HWO Spectra for a 10% O<sub>2</sub> PAL Case  
 Fig 8: Simulated HWO spectra for an exo-Earth with atmospheric profiles corresponding to 1 and 10% O<sub>2</sub> PAL cases. NEP values are taken for SiC versus other material and demonstrate the unique ability of SiC to enable access to the NUV signature on 3 day timescales.

Target SiC instrument parameters are taken from previous and current work and incorporated in PSG’s instrument module. An NEP value of 1E19 for SiC is taken from earlier SiC work<sup>3</sup> and is scaled based upon  $D^*/\text{NEP}$  values in figure 7, while an NEP value of 1E17 is used as a comparison value for other detectors such as AlGaIn and Si detectors.<sup>3</sup> The coronagraph model is based upon the PSG’s LUVOIR Extreme Coronagraph for Living Planetary Systems (ECLIPS) coronagraph model, with a modified 6.7m inscribed diameter for the telescope, a spectral resolution of  $R=7$  and

an exo-zodi level of 3 assumed for the system. A QE value of 0.8, emissivity of 0.2 and telescope temperature of 270K are taken from requirements for LUVOIR, and are all targets for current SiC development. Figure 8a and 8b show results for the two simulated cases (1 and 10% O<sub>2</sub> PAL) with a comparison of the performance of the different detectors. Total observation time for both cases is 3 days, which is chosen to achieve SNR of at least 3 for the increased flux due to ozone at the longer wavelengths in the better performing detector, which in both cases is SiC. The integration time and detector properties will vary as requirements are clarified, simulation parameters are optimized and fabrication and detector development progress is made. However, the general relationship from the two simulations is clear and robust - the potential dark current advantages that SiC may offer from similar packaging configurations is likely to yield more robust detections of potential signatures in the NUV, by at least an order of magnitude in SNR. Of note is that there are potential degeneracies with rayleigh scattering and aerosols in this spectral region, but there should be differences in the spectral signatures between those confounding sources versus ozone that the improved SNR may be able to leverage.

The improved noise performance that SiC may offer would translate to other potential UV instruments that HWO may baseline. While the format and design of such detectors would vary based upon the specific use cases, our team is examining potential applicability for different instruments. The improved noise performance and other characteristics of future SiC detectors would also be useful for other observational platforms in astrophysics and other disciplines. All of these potential use cases will benefit from additional technology and engineering advancement work that is informed by science modeling, including the work that our team is carrying out and will carry out in the near future as part of our ongoing projects.

### *Disclosures*

The authors declare that there are no financial interests, commercial affiliations, or other potential conflicts of interest that could have influenced the objectivity of this research or the writing of this paper.

### *Acknowledgments*

Our team acknowledges the following funding sources that supported the work detailed in the paper: NASA SBIR Contracts no. NNX12CA37C (2012), NNX15CG39P (2015), NNX17CG15C (2017), NNX17CG32P (2017), 80NSSC22PA995 (2022), 80NSSC23CA084 (2023), 80NSSC24CA054 (2024). This work was also supported by the NASA Space Technology Mission Directorate Early Career Initiative Program. The work was also supported by PICASSO grants 21-PICASSO21-0016 and Ultra-Violet Detector Innovation for Raman Exploration and Characterization (UV-DIRECT) of Ocean Worlds. The team also acknowledges support through Goddard's Internal Research And Development program. P.S. would like to acknowledge support from the Goddard Space Flight Center (GSFC) Sellers Exoplanet Environments Collaboration (SEEC), which is supported by the NASA Planetary Science Division's Research Program. R.W. would like to acknowledge support from the Future Investigators in NASA Earth and Space Science and Technology program.

### *References*

- 1 National Academies of Sciences, Engineering, and Medicine, *Pathways to Discovery in Astronomy and Astrophysics for the 2020s* (2021). Provided by the SAO/NASA Astrophysics Data System.

- 2 S. Tuttle, M. Matsumura, D. R. Ardila, *et al.*, “Ultraviolet Technology To Prepare For The Habitable Worlds Observatory,” *arXiv e-prints* , arXiv:2408.07242 (2024).
- 3 F. Yan, X. Xin, S. Aslam, *et al.*, “4h-sic uv photo detectors with large area and very high specific detectivity,” *IEEE Journal of Quantum Electronics* **40**(9), 1315–1320 (2004).
- 4 National Academies of Sciences, Engineering, and Medicine, *Origins, Worlds, and Life: A Decadal Strategy for Planetary Science and Astrobiology 2023-2032*, The National Academies Press, Washington, DC (2023).
- 5 J. T. Clarke, J. Ajello, J. Luhmann, *et al.*, “Hubble space telescope uv spectral observations of io passing into eclipse,” *Journal of Geophysical Research: Planets* **99**(E4), 8387–8402 (1994).
- 6 M. De Napoli, “Sic detectors: A review on the use of silicon carbide as radiation detection material,” *Frontiers in Physics* **10** (2022).
- 7 A. Ullah, M. R. Amirzada, M. D. R. Jahan, *et al.*, “Continuously varying thickness interference bandpass filter for the visible spectral range: Using ion beam sputter deposition,” *Advances in Materials Science and Engineering* **2022**(1), 8390315 (2022).
- 8 R. B. Rivera, “Astrophysics biennial technology report 2022,” tech. rep. (2022).
- 9 B. Dorsman, G. Raaijmakers, S. B. Cenko, *et al.*, “Prospects of Gravitational-wave Follow-up through a Wide-field Ultraviolet Satellite: A Dorado Case Study,” *The Astrophysical Journal* **944**, 126 (2023).
- 10 E. Schwieterman, C. Reinhard, S. Olson, *et al.*, “The Importance of UV Capabilities for Identifying Inhabited Exoplanets with Next Generation Space Telescopes,” *arXiv e-prints* , arXiv:1801.02744 (2018).

- 11 E. Spinei, A. Whitehill, A. Fried, *et al.*, “The first evaluation of formaldehyde column observations by improved pandora spectrometers during the korus-aq field study,” *Atmospheric Measurement Techniques* **11**(9), 4943–4961 (2018).
- 12 A. K. Sood, J. W. Zeller, P. Ghuman, *et al.*, “High performance GaN/AlGaN ultraviolet avalanche photodiode detector technologies,” in *Image Sensing Technologies: Materials, Devices, Systems, and Applications VI*, N. K. Dhar, A. K. Dutta, and S. R. Babu, Eds., **10980**, 109800M, International Society for Optics and Photonics, SPIE (2019).
- 13 S. Aslam, D. Franz, C. Stahle, *et al.*, “Dual band ultraviolet algan photodetectors for space applications,” in *2007 International Semiconductor Device Research Symposium*, 1–1 (2007).
- 14 S. Aslam, R. E. Vest, D. Franz, *et al.*, “External quantum efficiency of pt/n-gan schottky diodes in the spectral range 5–500nm,” *Nuclear Instruments and Methods in Physics Research Section A: Accelerators, Spectrometers, Detectors and Associated Equipment* **539**(1), 84–92 (2005).
- 15 S. Aslam, F. Yan, D. E. Pugel, *et al.*, “Development of ultra-high sensitivity wide-band gap UV-EUV detectors at NASA Goddard Space Flight Center,” in *Solar Physics and Space Weather Instrumentation*, S. Fineschi and R. A. Viereck, Eds., **5901**, 59011J, International Society for Optics and Photonics, SPIE (2005).
- 16 A. Akturk, N. Goldsman, S. Aslam, *et al.*, “Comparison of 4h-sic impact ionization models using experiments and self-consistent simulations,” *Journal of Applied Physics* **104**, 026101 (2008).
- 17 V. Strelakov, “Large-format algan pin photodiode arrays for uv images,” *NASA Tech Briefs* (2010).

- 18 X. Zhou, X. Tan, Y. Lv, *et al.*, “128-pixel arrays of 4h-sic uv apd with dual-frequency pecvd sin x passivation,” *Optics Express* **28**(20), 29245–29252 (2020).
- 19 Y. Lu, Y. Zhang, and X. yang Li, “Properties of InGaN P-I-N ultraviolet detector,” in *7th International Symposium on Advanced Optical Manufacturing and Testing Technologies: Optoelectronics Materials and Devices for Sensing and Imaging*, Y. Jiang, J. Yu, and B. Kippelen, Eds., **9284**, 92840P, International Society for Optics and Photonics, SPIE (2014).
- 20 M. Liao, “Progress in semiconductor diamond photodetectors and mems sensors,” *Functional Diamond* **1**(1), 29–46 (2022).
- 21 T. Chen, X. Gao, J.-Y. Zhang, *et al.*, “Ultrasensitive zno nanowire photodetectors with a polymer electret interlayer for minimizing dark current,” *Advanced Optical Materials* **8**(4), 1901289 (2020).
- 22 A. Jewell, J. Hennessy, T. Jones, *et al.*, “Ultraviolet detectors for astrophysics missions: a case study with the star-planet activity research cubesat (SPARC),” in *High Energy, Optical, and Infrared Detectors for Astronomy VIII*, A. D. Holland and J. Beletic, Eds., **10709**, 107090C, International Society for Optics and Photonics, SPIE (2018).
- 23 M. De Napoli, “Sic detectors: A review on the use of silicon carbide as radiation detection material,” *Frontiers in physics* **10**, 898833 (2022).
- 24 J. Herman and J. Mao, “Seasonal variation of total column formaldehyde, nitrogen dioxide, and ozone over various pandora spectrometer sites with a comparison of omi and diurnally varying dscovr-epic satellite data,” *EGUsphere* **2024**, 1–20 (2024).
- 25 P. Mackowiak, J.-M. Köszegi, M. Schneider-Ramelow, *et al.*, “Tsicv based silicon carbide

- interposer technology,” in *2023 Smart Systems Integration Conference and Exhibition (SSI)*, 1–6, IEEE (2023).
- 26 C. Sun, H. Guo, L. Yuan, *et al.*, “Bidirectional bias response ultraviolet phototransistors with 4h-sic npn multi-layer structure,” *IEEE Photonics Technology Letters* **34**(2), 81–84 (2022).
- 27 The LUVOIR Team, “The LUVOIR Mission Concept Study Final Report,” *arXiv e-prints* , arXiv:1912.06219 (2019).
- 28 J. E. Hylan, M. R. Bolcar, J. Crooke, *et al.*, “The large uv/optical/Infrared surveyor (luvoir): Decadal mission concept study update,” in *2019 IEEE Aerospace Conference*, 1–15, IEEE (2019).
- 29 N. J. Planavsky, C. T. Reinhard, X. Wang, *et al.*, “Low Mid-Proterozoic atmospheric oxygen levels and the delayed rise of animals,” *Science* **346**, 635–638 (2014).
- 30 E. Mamajek and K. Stapelfeldt, “Nasa exoplanet exploration program (exep) mission star list for the habitable worlds observatory (2023),” *arXiv preprint arXiv:2402.12414* (2024).
- 31 N. W. Tuchow, C. C. Stark, and E. Mamajek, “Hpic: The habitable worlds observatory preliminary input catalog,” *The Astronomical Journal* **167**, 139 (2024).
- 32 G. Cooke, D. Marsh, C. Walsh, *et al.*, “A revised lower estimate of ozone columns during earth’s oxygenated history,” *Royal Society open science* **9**(1), 211165 (2022).
- 33 G. L. Villanueva, M. D. Smith, S. Protopapa, *et al.*, “Planetary spectrum generator: An accurate online radiative transfer suite for atmospheres, comets, small bodies and exoplanets,” *Journal of Quantitative Spectroscopy and Radiative Transfer* **217**, 86–104 (2018).
- 34 P. Saxena, G. L. Villanueva, N. T. Zimmerman, *et al.*, “Simulating reflected light exoplanet spectra of the promising direct imaging target, *v* andromedae d, with a new, fast sam-

pling method using the planetary spectrum generator,” *The Astronomical Journal* **162**(1), 30 (2021).

## List of Figures

- 1 Micrographs from the process of different diode regions being defined by ion implantation for the tall, narrow aspect ratio diodes being developed for spectroscopy applications for the ECI program.
- 2 Micrographs from the process of different diode regions being defined by ion implantation for diode arrays with different pixel pitch for the PReSSiC project, targeting diode miniaturization.
- 3 The wafer-scale layouts for the PReSSiC project fabrication run (left) and the ECI program fabrication run (middle, right).
- 4 Previously fabricated photodiodes integrated with the first stage of a readout circuit on the same SiC die.
- 5 The structure of SiC photodiode-based focal plane arrays for the ECI effort consists of: (a) A core  $1 \times 1024$  array of SiC photodiodes, which fans out to wirebond pads matched to the inputs of wire bondable ROICs. In this case, the array is interfaced with 4 CTIA ROICs, each with 256 inputs. (b) The ECI effort is currently in the process of characterizing multiple diode variants, including: (i) arrays with a  $25 \mu\text{m}$  pitch, and (ii) arrays with a  $50 \mu\text{m}$  pitch.

- 6 Characterization of large format SiC photodiodes for ECI effort including (a) broad spectrum quantum efficiency characterization and (b) dark current measurement. Additional development work is expected to improve QE values though current values already satisfy Pandora-SiC goals, while dark current is an upper bound on the true value given measurement limitations.
- 7 Comparison of NEP and Specific Detectivity of SiC Diodes.
- 8 Simulated HWO spectra for an exo-Earth with atmospheric profiles corresponding to 1 and 10% O<sub>2</sub> PAL cases. NEP values are taken for SiC versus other material and demonstrate the unique ability of SiC to enable access to the NUV signature on 3 day timescales.

## List of Tables